Available online at www.sciencedirect.com

ScienceDirect

journal homepage: www.elsevier.com/locate/issn/15375110

Special Issue: Sensing and Control of Crop Water Status

Research Paper

Hyperspectral machine vision as a tool for water stress severity assessment in soilless tomato crop ☆

A. Elvanidi [a], N. Katsoulas [a,*], K.P. Ferentinos [b,1], T. Bartzanas [b], C. Kittas [a]

[a] University of Thessaly, Dept. of Agriculture Crop Production and Rural Environment, Fytokou Str., 38446, Volos, Greece

[b] Centre for Research and Technology Hellas, Institute for Research and Technology of Thessaly, Dimitriados 95 & P. Mela, 38333, Volos, Greece

ARTICLE INFO

Article history:
Published online 22 November 2017

Keywords:
Hyperspectral
Reflectance index
Crop water stress index
Machine vision
Reflectance index

Early detection of water deficit stress is essential for efficient crop management. In this study, hyperspectral machine vision was used as a non-contact technique for detecting changes in spectral reflectance of a soilless tomato crop grown under varying irrigation regimes. Four different irrigation treatments were imposed in tomato plants grown in slabs filled with perlite. The plants were grown in a growth chamber under controlled temperature and light conditions, and crop reflectance measurements were made using a hyperspectral camera to measure the radiation reflected by the crop from 400 nm to 1000 nm. The results showed that crop reflectance increased with increasing water deficit, and the detected reflectance increase was significant during the first day of irrigation was withheld. Based on the reflectance measurements, several crop indices were calculated and correlated with substrate volumetric water content and tomato leaf chlorophyll content. The results showed that when the modified red simple ratio tndex (*mrSRI*) and the modified red normalized vegetation index (*mrNDVI*) values increased by more than 2.5% and 23% respectively, the substrate volumetric water content decreased by more than 3%. In addition, when the Transformed Chlorophyll Absorption Reflectance Index (*TCARI*) value increased by about 16%, the leaf chlorophyll content decreased by about 3%. These results of the present study are promising for the development of a non-contact method for estimating plant water status in tomato crops grown under controlled environment.

☆ This paper has been developed from a paper presented at the ISHS symposium Sensing Plant Water Status, 5th – 7th October, 2016. The original conference paper will appear in the Proceedings of the First International Symposium on Sensing Plant Water Status – Methods and Applications in Horticultural Science (SPWS2016) to be published in Acta Horticulturae in 2018.

* *Corresponding author.*
E-mail address: nkatsoul@uth.gr (N. Katsoulas).

[1] Permanent Address: Dept. of Agricultural Engineering, Institute of Soil & Water Resources, Hellenic Agricultural Organization 'Demeter', 61 Dimokratias Av., 13561, Athens, Greece.

https://doi.org/10.1016/j.biosystemseng.2017.11.002
1537-5110/

1. Introduction

Biotic or abiotic factors may cause plant stress, affect plant growth and reduce productivity. Plant stress is expressed in the plant canopy in many types of symptoms. For example, plant stress caused by harsh microclimate conditions closes stomata and impedes transpiration, resulting in changes in leaf temperature (Katsoulas, Savvas, Tsirogiannis, Merkouris, & Kittas, 2009) but other symptoms of water deficit stress include morphological changes such as leaf curling or wilting due to loss of cell turgidity.

To avoid plant stress conditions, an optimal management of the aerial and root environment of the crop is needed. Usually, environmental conditions in greenhouses are monitored and managed by sampling at a single position, which is considered to be illustrative of average conditions, assuming a complete homogeneity of greenhouse microclimate. However, this hypothesis is not always valid since large temperature or humidity gradients do exist due to the variation of outside weather conditions but also to the greenhouse climate control systems per se, i.e. by the use of heating, insulation, ventilation or cooling systems (Kittas, Bartzanas, & Jaffrin, 2003; Max & Schurr, 2012). To avoid this, some climate and irrigation control systems propose the establishment of sensors at various locations inside the greenhouse (Ferentinos, Katsoulas, Tzounis, Bartzanas, & Kittas, 2017) or to manually perform measurements at different locations to adjust control strategies (Katsoulas et al., 2016).

Early detection of plant stress is critical especially in intensive production systems in order to minimise both acute and chronic loss of productivity. Direct and real-time monitoring of plant responses and processes under specific environmental and root conditions can help to improve climate and irrigation control and overall production over time and space. To achieve this, a sensing system equipped with a multi-sensor platform moving over the canopy needs to be developed by using plants as 'sensors' to communicate their actual state and needs.

Until recently, methods for the measurement of substrate water content for soilless crops or soil water tension and plant physiological factors, such as leaf water potential and sap flow, among others, to detect water deficit stress, were quite complex and problematic. They were limited to relatively small spatial scale, making their application to a commercial multi-sensor scale rather infeasible, requiring, in addition, physical contact with the plants or destructive sensing techniques (Alchanatis et al., 2010; Ray, Das, Singh, & Panigrahy, 2006). Current computational intelligence techniques have allowed the development of advanced systems such as the hyperspectral optic system that supplies information from a targeted object, which would facilitate the calculation of morphological (size, shape, texture), spectral (colour, temperature, moisture) and temporal data (growth rate, development, dynamic change of spectral and morphological states). Such a system can lead to the development of a real-time plant canopy health, growth and quality monitoring system, based on multi-sensor platforms (Story & Kacira, 2015).

The progress of ground-based reflectance measurement techniques has played a critical role in accurate monitoring and assessment of plant reflectance. Several sensor systems are available and many ground-based remote sensing (RS) technologies have been used to obtain the required information (Lan, Zhang, Lacey, Hoffmann, & Wu, 2009), but the improvement of non-imaging field spectroscopy to image RS data acquisition has led to the generation of a vast amount of plant reflectance data at higher spatial resolution (Liaghat & Balasundram, 2010). The new generation of ground-based imaging spectrometers already provides a considerable improvement in availability and accuracy of information on crop conditions, where information from RS imagery is being used for large scale irrigation policy level decision in the open field (Govender, Dye, Weiersbye, Witkowski, & Ahmed, 2009). Despite the cost and the complexity of hyperspectral techniques, reflectance can be a useful tool for early detection of water deficit stress, as it can measure plant reflectance remotely. However, reflectance measurements recorded by machine vision cannot be used directly as a metric of leaf water content, and that is why reflectance indices (RI) are used. An RI is results from the combination of data from two or more spectral bands, which are not influenced by the climatic conditions and sunlight, and could give more detailed information about plant water status. Then, having identifying representative RIs, simpler sensors measuring certain spectral bands could be used in real-time in a cost-effective manner.

Up to now, the majority of RI have been studied in the open field and in laboratory scale, and certainly not under covered structures. The objective of this work is to study commonly used RI and spectral regions [based on the list compiled by Katsoulas et al. (2016)] in hyperspectral RS techniques that can be applied for early water deficit stress detection under controlled environment conditions. The efficiency of spectral indices in detecting water is benchmarked with direct and indirect plant physiological measurements, such as leaf chlorophyll content and substrate water content. The applied objective of this work is to develop the methodology for irrigation scheduling decision-making based on crop reflectance data and simplified RI.

2. Materials and methods

2.1. Experimental set up

The experiments were carried out during January and February of 2015 in a controlled growth chamber located in Velestino, Central Greece, with a ground area of 28 m^2 (4 m × 7 m) and height of 3.2 m. Air temperature, relative humidity (*RH*), light intensity and CO_2 concentration were automatically controlled using a climate control computer (Argos Electronics, Greece). Air temperature and humidity were controlled by means of a heat exchanger while CO_2 concentration was controlled by adding pure CO_2. The light intensity was controlled using 24 high pressure sodium lamps, 600W each (MASTER GreenPower 600W EL 400V Mogul 1SL, Philips), operated in four clusters with six lamps per cluster. The clusters were turned on progressively during morning hours and switched off progressively in the evening to simulate the daily distribution of solar radiation. The average

irradiance when all 24 lamps were used was 240 W m^{-2} (about 350 μmol m^{-1} s^{-1}).

Tomato plants (*Solanum lycopersicum* cv. Elpida, provided by Spyrou SA, Athens, Greece) were grown in slabs filled with perlite (ISOCON Perloflor Hydro 1, ISOCON S.A., Athens, Greece). Two units comprising two crop lines each (six slabs per line, three plants per slab) were used.

Nutrient solution was supplied via a drip system and was controlled by a time-program irrigation controller (8 irrigation events per day, at 07:00, 10:00, 12:00, 14:00, 16:00, 18:00, 19:30 and 03:30, local time), with set-points for electrical conductivity at 2.4 dS m^{-1} and pH at 5.6.

The measurements started thirty days after transplanting, when the plants had about 10 leaves each, were about 1 m in height and had a leaf area index of about 0.8. In order to study the effects of irrigation water deficit on crop reflectance characteristics, four different irrigation treatments were applied for 24 days. Two treatments had a constant irrigation regime throughout the period:

(a) regularly irrigated plants, with 100% coverage of their water needs (control treatment: C100; irrigation dose of 120 mL per plant; 8 events per day),
(b) plants irrigated with 50% coverage of their water needs (C50; irrigation dose of 60 mL per plant; 8 events per day), and two rapid drought treatments, established by removing the drippers from the slabs and letting the slab dry progressively over several days, in plants that were previously:
(c) regularly irrigated with 100% coverage of their water needs (WS100) and
(d) irrigated with only 50% of their needs (WS50).

The plants of treatment (b) and (d) were only irrigated according to the time schedule irrigation program on the first day of the experiment (Day 1). From then on, the plants in treatment (b) and (d) were irrigated with 50% coverage of their water needs. In addition, in treatment (c) and (d) the drippers were removed from the slabs for several days; in treatment (c) during the Days 4–8 and 18–22 and in treatment (d) during the Days 4–7 and 18–21. After that period the drippers were placed back in the slab and the relevant basic irrigation treatment resumed.

In hydroponic crops, it is not possible to obtain water deficit (when withholding irrigation completely) without affecting also the availability of nutrients in the root zone. Thus, the effect on spectral reflectance observed in the water deficit stressed plants may be the combination of both water and nutrient stress. Nevertheless, considering that each water deficit treatment lasted only 5 days and taking into account that for very mobile nutrients such as nitrogen and potassium, deficiency symptoms develop predominantly in the older and mature leaves (Taiz, Zeiger, Møller, & Murphy, 2015) and that the measurements in the present study were made in young and fully developed leaves, it could be considered that the symptoms detected were mainly due to water deficit stress. This was also the methodology followed in similar prior studies (e.g. Sarlikioti, Driever, & Marcellis, 2010).

2.2. Measurements

Air temperature (T, °C) and relative humidity (RH, %) were measured using two temperature-humidity sensors (model HD9008TR, Delta Ohm, Italy) calibrated before the experimental period, placed 1.8 m above ground level. Using the T and RH values, the air vapour pressure deficit values were calculated. Irradiance ($R_{g,i}$, W m^{-2}) inside the growth chamber was recorded using a solar pyranometer (model SKS 1110, Skye instruments, Powys, U.K.) located 1.8 m above ground. Substrate volumetric water content (θ, %) was estimated using capacitance sensors (model WCM, Grodan Inc., The Netherlands). Three water content sensors were placed horizontally in the middle (height and width) of the hydroponic slabs (one each in C100, WS100 and WS50 treatments). The above data were automatically recorded in a data logger system (Zeno 3200, Coastal Environmental Systems Inc., Seattle, WA, USA). Measurements were performed every 30 s and 10-min average values were recorded.

The plant leaf chlorophyll content was measured using non-destructive sensing by means of an Opti-Science sensor performing measurements in contact with the leaf (CCM 200, Opti-Science, NH, USA). Measurements were taken in 45 young and fully developed leaves per treatment per day. The values recorded by means of the CCM 200 sensor were correlated with chlorophyll-a (Chl_a) and chlorophyll-b (Chl_b) values (μg cm^{-2}) obtained in the lab for the same set of leaves using Lichtenthaler and Wellburn (1983) protocol.

The hyperspectral camera Imspec V10 (Spectral Imaging Ltd, Finland) was used to obtain reflectance measurements of the tomato plants. The camera operates in the visible and near infrared (VNIR) spectrum region between 400 and 1000 nm (spectral resolution: 2.8 nm; spectral resolution FWHM (full width at half maximum): 3.0 nm (30 μm slit); spectral sampling: 0.78–6.27 nm per pixel; spatial resolution: 1312 pixels; frame rate: 65 fps, up to 185 fps with binning) and included a 12 bit CMOS-type sensor. The camera system was placed on a moving cart, so that images of the vertical canopy axis could be obtained.

The hyperspectral imaging system was calibrated inside the growth chamber. For extra illumination of the target area (70 × 100 cm), four quartz-halogen illuminators (500 W each) were used to provide calibration wavelengths from 400 to 900 nm. For optimal radiometric calibration of the imaging system, a calibration protocol was followed in two steps. The first step was performed in the laboratory, using known light sources and the second step of the calibration was performed in the controlled growth chamber. Katsoulas, Elvanidi, Ferentinos, Bartzanas, and Kittas (2014), Katsoulas et al. (2016) and Elvanidi, Katsoulas, Bartzanas, Ferentinos, and Kittas (2017) have given more information about the calibration procedures followed.

The camera was located at a constant distance of 1 m from the vertical axis of the canopy (Fig. 1a) to sample the canopy area of young, fully developed leaves between the 3rd and 6th branch of three plants. At the time of measurements, a black surface was used as background, in order to block out any reflection from growth chamber surfaces, ensuring a constant field of view without shadows.

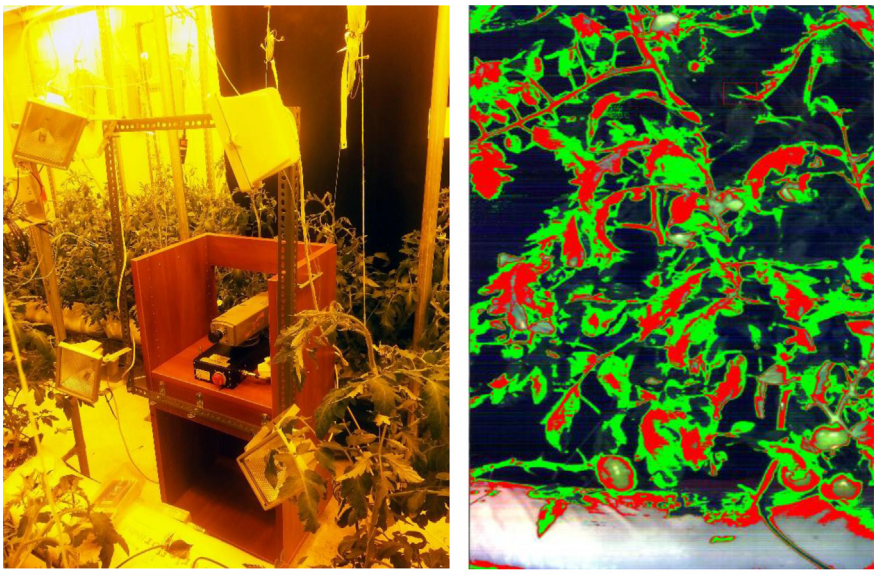

(a) (b)

Fig. 1 – (a) Hyperspectral imaging system into growth chamber. (b) Red and green plant's region of interest based on 2 class *k*-means method before the mask process of the image. (For interpretation of the references to colour in this figure legend, the reader is referred to the web version of this article.)

To further overcome the reflection differences due to shadows and reflections and measure true reflectance, a white low-density polyethylene sheet of known reflectance (W) was positioned 1 m in front of the sensor and its measured reflectance served as a normalising reference for all readings. Before each calibration (steps one and two described above) or measuring process, dark images were additionally acquired, by covering the lens with a cap. Plant reflectance (R) was calculated as the ratio of the difference between actual image reflectance (r, i.e. the intensity of reflected light signal in a certain bandwidth) and dark reference (D) to the difference of white and dark references ($R = (r - D)/(W - D)$) (Polder, van der Heijden, Keizer, & Young, 2003).

A sample of three images per treatment per hour between 8:00 and 16:00 was taken and the mean reflectance values of the area of interest were calculated. Before that, image segmentation was performed to segment leaves from the background using isodata and k-means statistical methods. After segmentation, a mask was created on the area covered by the young and fully developed leaves. The mask was applied to all other bands of the hyperspectral image to extract the mean intensity value of the relevant leaf area. MATLAB (by MathWorks®, Inc., Natick, MA, USA, version R20150) and ENVI (by Exelis®, Visual Information Solutions, Inc., USA) software packages were used for image analysis and plant reflectance acquisition (Fig. 1b).

The measurements were separated into two periods (repetitions). The first period lasted 10 days (Day 1–10) and the second period 9 days (Day 16–24). No reflectance data were recorded during the intermediate days of the two periods (Days 11–15) due to sensor recalibration.

2.3. *Calculations*

Based on the available reflectance measurements, the following indices were calculated and evaluated to explore their relationship with water deficit stress (Table 1). The average band indices (AB) reported in Table 1, were estimated by the mean reflection of a specific spectral region.

2.4. *Statistical analysis*

Comparison of means was performed by applying one-way ANOVA (analysis of variance) at a confidence level of 95% ($p \leq 0.05$) using SPSS (Statistical Package for the Social Sciences, IBM, USA). To compare the plant reflectance values between treatments, the reflectance data were grouped in 196 groups (bands of 3.06 nm each) from 400 to 1000 nm. One-way ANOVA was applied to each band to identify the bands with statistically significant differences between treatments. One-way ANOVA was also used to compare the daily mean values of the RI between the plants of the different treatments.

Additionally, linear regression was performed between the studied RI and some abiotic parameters. The mean values and the measurement variability (standard error of the mean, ±SE or standard deviation, ±SD) of the parameters are reported. The letter "n" is used to designate the daily sample size of each parameter (θ, R, Chl) per treatment (n: number of samples per day per treatment).

Furthermore, a classification tree (CT) was used to create a tree-based prediction model. Based on CT methodology, prediction rules were used to predict future irrigation events. The CT developed was based on the classification regression tree

Table 1 – Spectral indices evaluated in this study (c.f. Katsoulas et al., 2016).

Acronym	Type index	Index name	Index formula
AB	Average band	Blue	B = 400–500
		Green	G = 500–600
		Red	R = 600–700
		Red near infrared	rNIR = 700–800
		Middle near infrared 1	mNIR 1 = 800–900
		Middle near infrared 2	mNIR 2 = 900–1000
SR	Simple ratio	Water index	$WI = R_{970}/R_{900}$
		Vogelman red edge index 1	$VOGREI\ 1 = R_{740}/R_{720}$
ND	Normalized difference	Photochemical reflectance index	$PRI = (R_{531} - R_{570})/(R_{531} + R_{570})$
		Similar photochemical reflectance index	$sPRI = (R_{560} - R_{510})/(R_{560} + R_{510})$
		Normalized difference vegetation index	$NDVI_{(490-620)} = (R_{490} - R_{620})/(R_{490} + R_{620})$
			$NDVI_{(800-680)} = (R_{800} - R_{680})/(R_{800} + R_{680})$
			$NDVI_{(710-810)} = (R_{710} - R_{810})/(R_{710} + R_{810})$
			$NDVI_{(790-670)} = (R_{790} - R_{670})/(R_{790} + R_{670})$
		Red normalized difference vegetation index	$rNDVI = (R_{750} - R_{705})/(R_{750} + R_{705})$
		Vogelman red edge index 3	$VOGREI\ 3 = (R_{734} - R_{747})/(R_{715} + R_{720})$
		Similar normalized difference vegetation index 1	$sNDVI\ 1 = (R_{810} - R_{710})/(R_{810} + R_{710})$
		Similar normalized difference vegetation index 2	$sNDVI\ 2 = (R_{810} - R_{560})/(R_{810} + R_{560})$
		Modified red simple radio index	$mrSRI = (R_{750} - R_{445})/(R_{705} - R_{445})$
		Modified red normalized difference vegetation index	$mrNDVI = (R_{750} - R_{705})/(R_{750} + R_{705} - 2^{*}R_{445})$
		Transformed chlorophyll absorption in reflectance index	$TCARI = 3[(R_{700} - R_{670}) - 0.2^{*}(R_{700} - R_{550})^{*}(R_{700}/R_{670})]$

method (CRT) to control the maximum number of levels of growth beneath the root. The model developed was calibrated (using training data) and validated (on a different set of data). The training sample set included 75% of the total (n = 76 data sets) daily reflectances for both experiment periods and the remaining 25% was used as a test sample. The training set was used to build the classification model, which was subsequently applied to the test set, which consists of records with unknown class labels. Each partition was marked as class label as either C (Control) or WS (Water Deficit Stress) to answer the question whether the crop was under water deficit stress. Thus, it could be considered that "C" is referred to "*no stressed plants/no irrigation is needed*" while "WS" is referred to the "*water deficit stress plants/irrigation is needed*". The tree is constructed from a given set of attributes such as θ, *Chl*, Photochemical reflectance index (*PRI*), Modified red normalized vegetation index (*mrNDVI*), Transformed Chlorophyll Absorption Reflectance Index (*TCARI*). The model was built according to substrate water content evolution, in which θ values lower than 39% have been defined as "WS". The algorithm employed a greedy strategy to grow the decision tree by making a series of locally optimal decisions about which attribute to use for partitioning data. According to this definition, the *mrNDVI* and *PRI* were defined as the discrete attributes and the irrigation definition was the prediction attribute. Each node of training or testing sample shows the predicted value, which is the mean value for the dependent variable at that node. The goal of the classification model was to predict the class label of the unknown records. Loh (2011) and IBM SPSS Statistics 21 guide (2012) give more information about each step in the procedure for exploratory and confirmatory classification analysis.

3. Results

The mean values of air temperature inside the growth chamber during the period of measurements were 22 °C and 17 °C for day and night-time periods, respectively, with small variations around these values. In addition, the mean values of air RH during the same time periods were 60% and 80%, respectively.

The daily average volumetric water content values of the substrate (θ, %) measured in the different treatments ranged between 35% and 42% (n = 54 per day per treatment). During the daytime period, the observed values of θ in the C100 treatment were at field capacity levels (about 40%–42%; ±SD = 1.06, ±SE = 0.24) (Fig. 2a). Compared to C100, the θ values in C50 and WS50 treatments decreased by more than 2.2% once the mild time-based irrigation was applied (Day 2). In addition, θ decreased rapidly ($p < 0.05$) during the first days of irrigation withholding (Day 4 & Day 18) once the drippers were removed from the slabs (by 3.0% and 3.4% in case of the plants of WS100 treatment, and 11.2% and 7.4% in case of the plants of WS50 treatment, in the 1st and 2nd Period, respectively). The slab water content reduction proceeded at a slower rate during the following days of irrigation withholding (Fig. 2a), reaching below 36% (±SD = 1.31; ±SE = 0.30). The θ values observed in the plants of WS100 treatment increased again as soon as the drippers were placed back to the slabs (Day 9, Day 23) while for the case of WS50 an increase of θ values was observed two days later.

The correlation between the values recorded by means of the CCM 200 sensor with chlorophyll-a (*Chl_a*) and chlorophyll-b (*Chl_b*) values (μg cm^{-2}) followed a linear regression equation of first order:

$$Chl\_a = 0.374\ CCI + 16.34,\ R^2 = 0.91,$$

$$Chl\_b = 0.089\ CCI + 4.75,\ R^2 = 0.86,$$

where CCI are the values recorded by the CCM 200 sensor. The chlorophyll_a content values (*Chl_a*, μg cm^{-2}) observed in C100

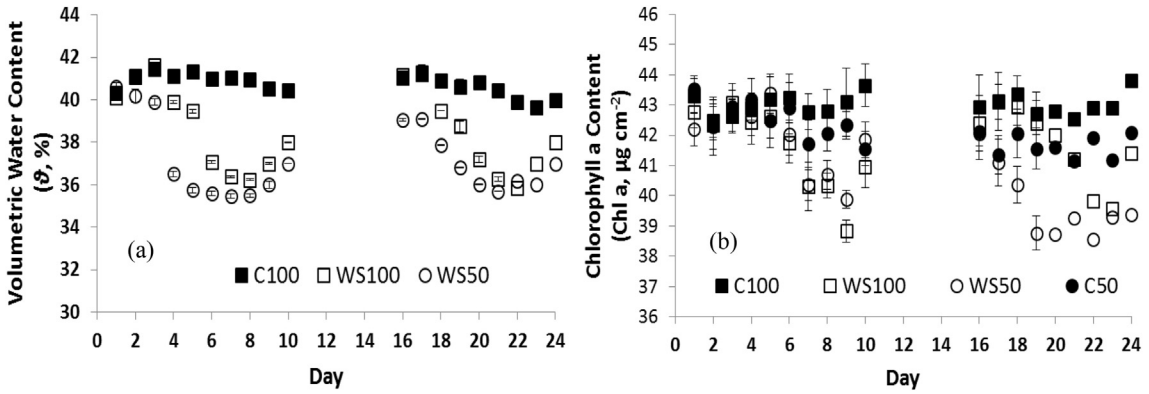

Fig. 2 – Evolution of (a) substrate volumetric water content values (θ, %) measured in the perlite slabs (n = 54) and (b) leaf chlorophyll content values (*Chl_a*, µg cm^{-2}) (n = 45) in the plants of the different treatments. Error bars represent the standard error (±SE) of the means.

plants showed stable chlorophyll content values (about 42–43 µg cm^{-2}; SE of ±0.80), (Fig. 2b). C50 plants showed a *Chl_a* reduction (2.5%, $p < 0.05$) six days after treatment initiation (Day 7). The plants of the rapid drought deficit treatment (Day 6 & 20 in case of WS100 treatment and Day 6 & 18 in case of WS50 treatment) influenced leaf chlorophyll content too, especially at the end of irrigation withholding cycle, reaching *Chl_a* values below 40 µg cm^{-2} (±SD < 5.50; ±SE < 0.80). The *Chl_a* values did not immediately recover when the irrigation was restarted but did on the last day of measurements. The *Chl_b* values observed in non-stressed plants were about 10.9–11.1 µg cm^{-2}, while the values observed in stressed plants followed similar evolution to that of *Chl_a*.

3.1. *Diurnal crop reflectance*

The spectral reflectance of tomato leaves from all treatments were similar (Fig. 3a) for the first days of the experimental period (Days 1–3). Thereafter, the reflectance in the near infrared (*NIR*) spectral region tended to increase as θ values were reduced

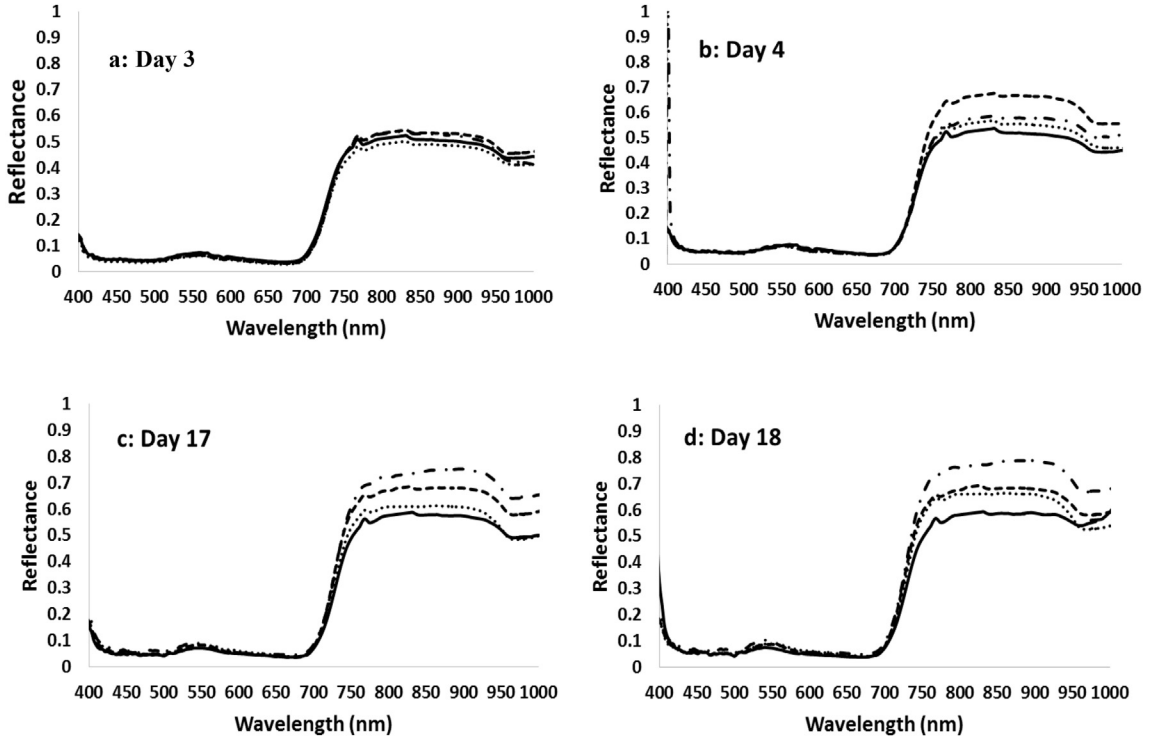

Fig. 3 – Evolution of leaf reflectance *R* of four different treatments (n = 27/day/treatment), during the period of measurements. Continuous line: C100; dash line: WS50, dotted line: WS100; dotted-dash line: C50.

progressively ($p > 0.05$), while the visible (*VIS*) spectral region remained stable throughout the period considered.

The reflectance values observed in the plants of the C50 treatment appeared not to be significantly affected by the irrigation treatment applied until Day 4, i.e., three days after the irrigation was reduced by 50%. However, the reflectance values were significantly increased in the *NIR* region from 770 nm to 952 nm, and remained high during the following days (Days 7–24). Further water deficit progress in the plant of C50 treatment resulted in significant reflectance increases between 451 nm and 554 nm and between 660 and 770 nm (from Day 9 and after). The same holds for the reflectance observed for the plants of WS50 treatment, as the values significantly increased (by up to 20%) only when the θ decrease reached 11%, following the drippers being removed from the slabs (Day 4) (Fig. 3b). The reflectance values measured for the plants of WS100 treatment significantly increased by up to 11% once θ had decreased by more than 4.5% ($p < 0.05$) (Day 5; $\theta = 39\%$). In any case, the reflectance values observed for the plants of both rapid water deficit treatments (WS100 and WS50 treatment) remained high during the irrigation withholding period and recovered as soon as the irrigation drippers were replaced in the slabs (Day 9 and Day 8, respectively), although θ values were still low.

From Fig. 3 and the statistical analysis, the spectral bands which were affected by the irrigation regime can be identified. The spectral region most sensitive to the effect of water deficit stress was between 700 nm and 1000 nm and more specifically between 835 nm and 922 nm. The reflectance curve in this region appeared to vary considerably, from the early days of irrigation differences. An increase of the reflectance curve in spectral regions lower than 700 nm (451 nm–554 nm and 640 nm–670 nm) was also observed, while crop water deficit stress increased. The region of the spectrum between 554 nm and 640 nm increased only when the plant water deficit stress was visible to the naked eye.

3.2. *Reflectance indices*

The measured values of leaf reflectance obtained with the hyperspectral camera were used for to estimate the RI (Table 1).

The *PRI* values observed in the plants of the control treatment (C100) varied between −0.086 and 0.012 (SD = ±0.034, SE = ±0.006) (Fig. 4a). No differences were observed in the *PRI* values of the four treatments during the Days 1–3. The *PRI* values increased as soon as θ was reduced by more than 4.5–5.0%. Contrary to *PRI* evolution, the *sPRI* values observed in the plants of WS100 treatment were significantly different from those observed in the plants of the control treatment as soon as θ differences were higher than 3% (after Day 7).

The *mrNDVI* (Fig. 4b) and modified red simple radio index (*mrsRI*) values observed in C100 varied from 0.82 to 0.85 (SD = ±0.01, SE = ±0.003) and 8.76 to 12.12 (SD = ±0.75, SE = ±0.17), respectively, following θ evolution.

TCARI values did not correlate with θ values. The *TCARI* values varied between 0.09 and 0.11 (SD = ±0.009, SE = ±0.002)

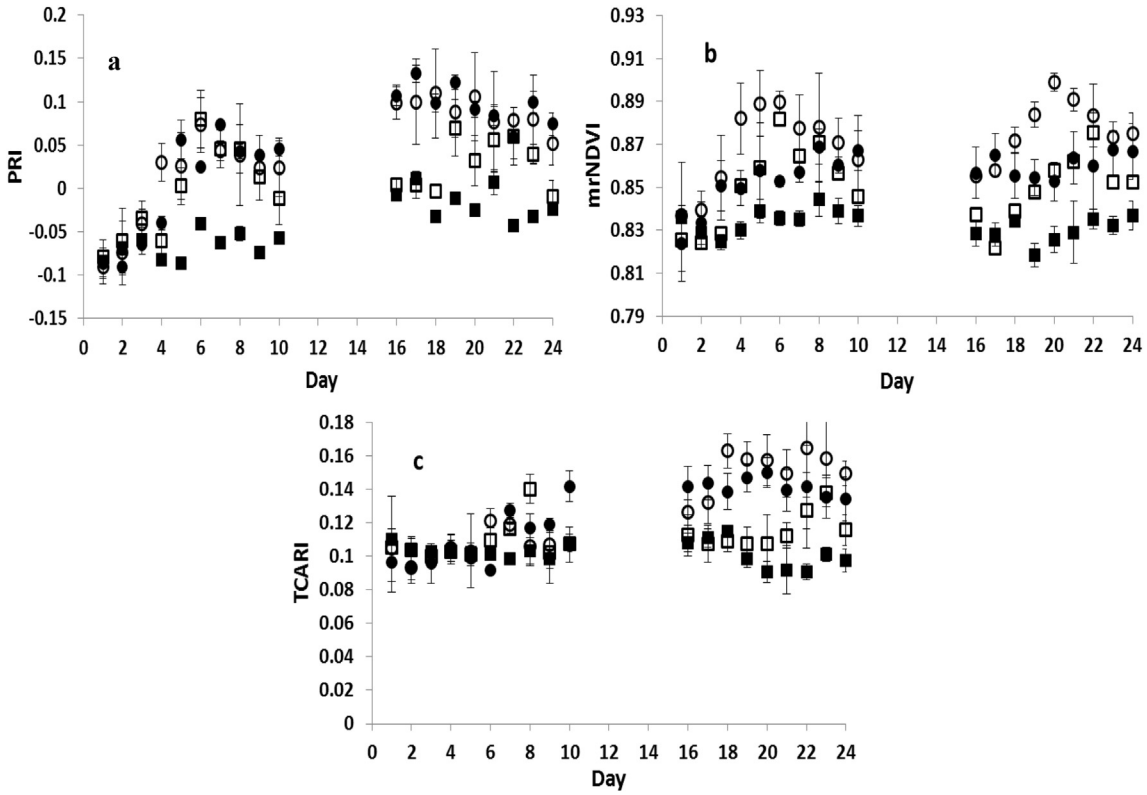

Fig. 4 – Evolution of (a) *PRI*, (b) *mrNDVI* and (c) *TCARI* values (n = 27/day/treatment) of the four treatments, during the period of measurements. Squares: C100 and WS100; circles: C50 and WS50; solid symbol: C100 and C50; empty symbol: WS100 and WS50. The error bars represent the standard deviation of the means.

whilst the *Chl_a* values were close to 42 μg cm^{-2} (during the irrigation period) and increased to 0.15 when θ was reduced to about 36% (Fig. 4c). Similarly, Vogelman red edge index 1 (*VOGREI 1*) values indicated the existence of plant water deficit stress when θ values were less than 38%.

Nonetheless, for the same value of θ observed in the plants of four irrigation treatments, different values of *PRI*, *sPRI*, *mrSRI* and *mrNDVI* were observed. Thus, in order to eliminate the effect of reflectance evolution over time, the differences between the index values of the treated (C50, WS50 and WS100) and control plants (C100) [Δindex(Treatment-Control)] were correlated with the volumetric water content and leaf chlorophyll content differences between the relevant treatments during the same time period [$\Delta\theta$ *or* $\Delta Chl\_a/b$(Treatment-Control)]. The coefficient of determination (R^2) obtained by the linear regression relationship for the difference in studied RI values observed between control and treated plants compared with the respective difference in *Chl_a/b* and θ values, is listed in Table 2. By plotting Δindex *vs* $\Delta\theta$ values and Δindex *vs* $\Delta Chl\_a/b$, linear relationships were found:

$$\Delta mrNDVI = 0.014\ \Delta\theta - 0.0023, \text{ with } R^2 = 0.80,$$

$$\Delta mrSRI = 1.0224\ \Delta\theta + 0.7452, \text{ with } R^2 = 0.82,$$

$$\Delta PRI = 0.022\ \Delta\theta + 0.0051, \text{ with } R^2 = 0.74,$$

$$\Delta sPRI = -0.021\ \Delta\theta + 0.0053, \text{ with } R^2 = 0.63,$$

$$\Delta TCARI = -0.0132\ \Delta Chl\_a - 0.0012, \text{ with } R^2 = 0.71,$$

$$\Delta TCARI = -0.0589\ \Delta Chl\_b + 0.0023, \text{ with } R^2 = 0.65,$$

$$\Delta VOGREI\ 1 = 0.0555\ \Delta Chl\_a - 0.0224, \text{ with } R^2 = 0.50,$$

$$\Delta VOGREI\ 1 = 0.2623\ \Delta Chl\_b - 0.0319, \text{ with } R^2 = 0.52.$$

3.3. Automation of water deficit stress detection

The CT developed using the training set had seven nodes (three nodes with at least one child and four nodes without children) (Fig. 5). In this tree, the predicted category is the detection of water deficit stress ("C" or "WS"). For each node, there is a table that provides the number (*n*) and the percentage (*%*) of "C" or "WS" cases in each RI category set as a dependent variable. Moreover, the category with highest count in each node is highlighted.

It was calculated that there was no water deficit stress when *mrNDVI* was ≤0.8456, thus "C" was returned (no irrigation is needed). Since there are no child nodes below it, this is considered as terminal node.

On the other hand, if the *mrNDVI* was greater than 0.8456, the *PRI* readings (next best predictor) had to be taken into consideration to identify water deficit stress and the node 2 shall be omitted. In this case, when *PRI* readings were ≤0.048, two values of the independent variable PRI merged into this single node. In particular, the sample of the plants that returned "C" (47.8%) was almost equal to those of "WC" (52.2%). According to this result, it is not clear whether the plants were under water deficit stress or not. This was also confirmed by the relevant node of the testing CT (Fig. 5b), where two independent values were merged into a single node too. In contrast to node 3 of training tree, in testing the majority of the sample (66.7%) returned "C". On the other hand, when *PRI* was higher than 0.048, 91.7% of the sample were characterised as water deficit stressed (the risk predicted by the model was not significant).

The predicted percent of the training sample was 86.7% indicating that the model classified approximately 86.7% of the irrigation events correctly. The classification result did, however, reveal one potential problem with this model: for those plants cultivated under water deficit stress, it predicted "WS" for 74% of them, which means that 26% of stressed plants were inaccurately classified with the "C" no-stress plants. On the other hand, only 5.4% of no-stress plants were inaccurately classified with the "WS" stressed plants. However, the finally estimation risk of misclassification of the training model was low at 13.3%. Similar to training tree, the testing tree classified 80% of stress type correctly, while the estimation risk was at 20%.

Table 2 – Coefficient of determination (R^2) obtained by linear regression of the difference in studied RI values observed in control and treated plants against the respective differences in *Chl_a*, *Chl_b* and θ values, for both experimental periods (*p < 0.05).

Index/Factors	ΔChl_a	ΔChl_b	Δθ	Index/Factors	ΔChl_a	ΔChl_b	Δθ
WI	0.01	0.01	0.01	rNDVI	0.01	0.14	0.08
VOGREI 1	0.5*	0.52*	0.15	VOGREI3	0.12	0.14	0.06
PRI	0.17	0.15	0.74*	sNDVI1	0.16	0.21	0.1
SPRI	0.16	0.12	0.63*	sNDVI2	0.11	0.19	0.03
$NDVI_{(490-620)}$	0.01	0.03	0.01	mrSRI	0.17	0.19	0.82*
$NDVI_{(800-680)}$	0.1	0.01	0.01	mrNDVI	0.31	0.37	0.8*
$NDVI_{(790-550)}$	0.01	0.01	0.4	TCARI	0.71*	0.67*	0.24

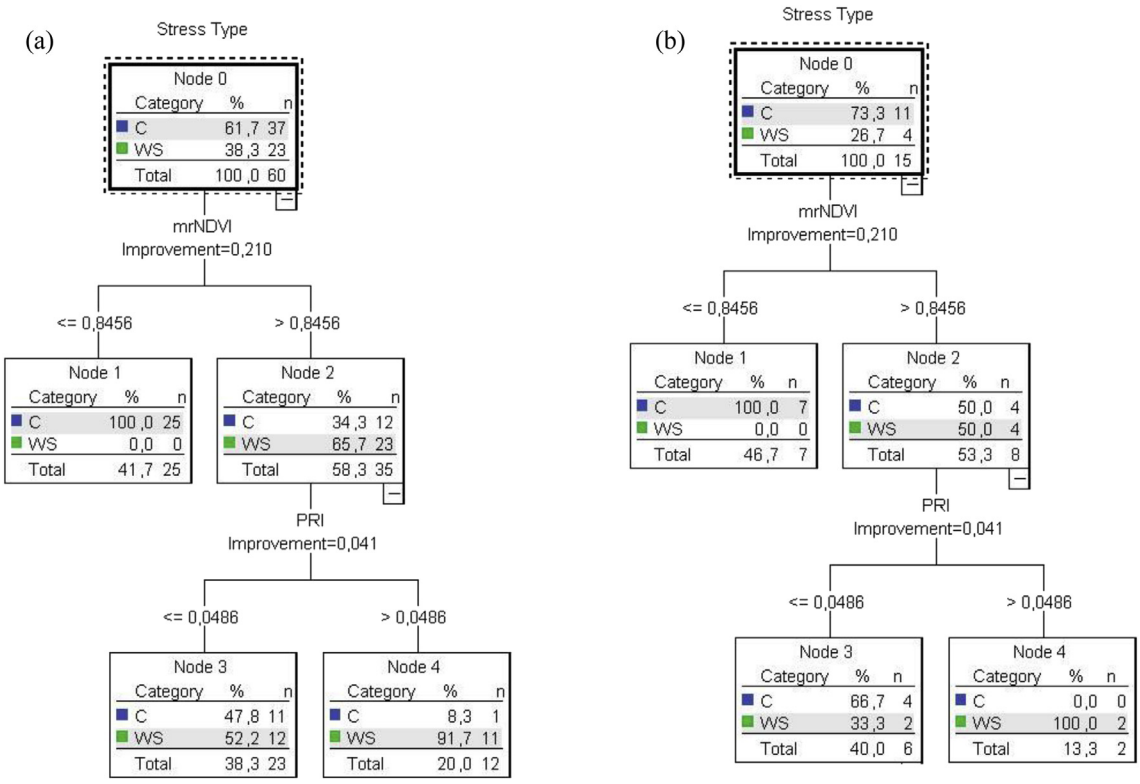

Fig. 5 – Classification Tree (CT) of (a) training sample for calibration and of (b) testing sample for validation. C: control plants; WS: water deficit stress plants.

4. Discussion

The volumetric water content of the substrate is a factor regularly used in the literature for indication of water deficit stress imposed on plants (Amatya, Manoj, & Alva, 2014; Kacira, Sase, Okushima, & Ling, 2005; Kim, Glenn, Park, Ngugi, & Lehman, 2010; Tsirogiannis, Katsoulas, Savvas, Karras, & Kittas, 2013). Low θ results in stomatal closure and leaf temperature increase, leading to diminishing of photosynthesis rate and leaf chlorophyll content (Baker & Rosenqvist, 2004; Lichtenthaler & Babani, 2000; Sarlikioti et al., 2010; Zarco-Tejada et al., 2013), and this was also confirmed in the present work. According to Genc, Inalpulat, Kizil, Mirik, Smith, and Mendes (2013), a decrease in leaf chlorophyll content in water deficit stressed plants provided evidence that water deficiency degraded the photosynthetic pigments and changed the leaf morphology in sweet corn canopies. However, the observed reduction in leaf chlorophyll content may be due to chloroplast movement during water deficit stress (Hoel & Solhaug, 1998).

The results presented in this work indicate that the water status differences among the plants of the different treatments were directly linked to changes in crop radiation reflectance. The spectral region most sensitive to the effect of water deficit stress was found to be between 700 nm and 1000 nm with special emphasis in the region between 835 nm and 922 nm. An increase of the reflectance in the region between 451 nm–554 nm and 640 nm–670 nm was also observed with the progress of plant water deficit stress development. These observations are in agreement with Köksal et al. (2011) and Schlemmer, Francis, Shanahan, and Schepers (2005) who determined similar increases of reflectance under water deficit stress in beans and maize.

Although the results observed in the *NIR* spectral region could potentially be used in quantifying crop water status, this relationship was weak and sometimes not significant when considered over the entire range of substrate water content values.

The results of the statistical analysis illustrated that *mrNDVI* and *mrSRI* can effectively estimate water deficit stress response by varying gradually from the onset to the end of the water deficit stress cycle. Indeed, when θ changed by more than 3.0% or 10%, *mrNDVI* and *mrSRI* varied more than 2.5% or 7% and 23% or 29% respectively. Similar findings have been presented by Amatya, Karkee, Alva, Larbi, and Adhikari (2012), who found increases of *mrNDVI* and *mrSRI* under water stress conditions.

Previous research has indicated that *PRI* is a sensitive indicator of water deficit stress (Peñuelas, Gamon, Fredeen, Merino, & Field, 1994; Sun et al., 2008; Suárez, Zarco-Tejada, Berni, González-Dugo, & Fereres, 2009; Sarlikioti et al., 2010). The results of the present study showed that as θ decreased, *PRI* also varied in a similar pattern, as long as the substrate water content decreased by more than 5.0%. Similar findings were observed by Sun et al. (2008). Gamon, Serrano, and Surfus (1997) mentioned that *PRI* was originally developed to estimate rapid changes in the water deficit stress cycle.

TCARI based on reflectance radiation at 550 nm, 670 nm and 700 nm has been considered suitable for detection of differences in reflectance between healthy and powdery mildew diseased plants (Gröll, Graeff, & Claupein, 2007). In recent years, *TCARI* has been studied as a RS indicator for chlorophyll measurement too (Lu et al., 2015). In this research, when *Chl_a* decreased by 2.9% then *TCARI* increased by 16.3%. The *VOGREI 1* is commonly used to correlate the reflectance at 720 nm and 740 nm with total chlorophyll content variation at leaf level due to water deficit stress effect (Vogelmann, Rock, & Moss, 1993). However, Amatya et al. (2012) found good correlation between *VOGREI 1* and soil water content too, two months after treatment initiation, by applying different irrigation doses (10%, 15%, 20% and 25% of field capacity). In the present study, the coefficient of determination of the correlation between *VOGREI 1* and θ or *Chl_a* was less than 0.5.

Genc et al. (2013) supported the CT as a very useful model to analyse complex data sets by providing visual results about plant water deficit stress deficit. In order to determine the water deficit stress severity, RI were investigated in CT paths. Among the indices, the CT model selected *mrNDVI* as a starter index to predict the water deficit stress. The CT analysis revealed that classification accuracy for the training sample was 84.2% and for the testing tree was 78.9%.

The overall success rate of classification between predicted and measured values of stressed tomato indicated that *mrNDVI* has potential to determine water deficit stress and CT algorithms have good potential in the classification of remotely sensed spectral data. However, the improvement in the performance of the decision tree classification approach with increases in the data set further strengthened the belief that model performance could probably be further improved with larger datasets.

5. Concluding remarks

The results of the present study confirmed that crop reflectance increases under crop water deficit stress. The *mrSRI* and the *mrNDVI* were identified as the two most relevant and sensitive indices to indicate water deficit stress. In addition, *TCARI* was strongly correlated with tomato leaf chlorophyll content variations. The CT algorithm trained in this work was successful in detecting crop water deficit stress through image analysis. These results are promising for the development of a non-contact method to assess plant water status in tomato crops grown under controlled environment, something that could aid in the better management of climate and irrigation control systems. Nevertheless, it has to be noted that the results presented correspond to just a twenty day period and the correlations observed are relevant to the conditions of the measurements and the specific crop studied.

Acknowledgments

This work has been co-financed by the European Union and Greek National Funds through the Operational Program "Education and Lifelong Learning" of the National Strategic Reference Framework (NSRF) – ARISTEIA "GreenSense" project (grant number 2632).

The authors would like to thank Dr Eftymia Levizou, Assistant Professor of the University of Thessaly for her help in leaf chlorophyll content measurements in the lab.

REFERENCES

Alchanatis, V., Cohen, Y., Cohen, S., Moller, M., Sprinstin, M., & Meron, M. (2010). Evaluation of different approaches for estimating and mapping crop water status in cotton with thermal imaging. *Precision Agriculture, 11*, 27–41. https://doi.org/10.1007/s11119-009-9111-7.

Amatya, S., Karkee, M., Alva, A. K., Larbi, P., & Adhikari, B. (2012). Hyperspectral imaging for detecting water stress in potatoes. *American Society of Agricultural and Biological Engineers, 12*, 1345197.

Amatya, S., Manoj, K., & Alva, A. K. (2014). Identifying water stress in potatoes using leaf reflectance as an indicator of soil water content. *Journal of Agricultural Engineering, 1*, 52–61.

Baker, N. R., & Rosenqvist, E. (2004). Applications of chlorophyll fluorescence can improve crop production strategies: An examination of future possibilities. *Journal of Experimental Botany, 55*, 1607–1621. ISSN 0022-0957.

Elvanidi, A., Katsoulas, N., Bartzanas, T., Ferentinos, K. P., & Kittas, C. (2017). Assessment of crop water status by means of crop reflectance. *Acta Horticulturae, 1164*, 297–304.

Ferentinos, K. P., Katsoulas, N., Tzounis, A., Bartzanas, T., & Kittas, C. (2017). Wireless sensor networks for greenhouse climate and plant condition assessment. *Biosystems Engineering, 153*, 70–81.

Gamon, J. A., Serrano, L., & Surfus, J. S. (1997). The photochemical reflectance index: An optical indicator of photosynthetic radiation use efficiency across species, functional types, and nutrient levels. *Oecologia, 112*, 492–501.

Genc, L., Inalpulat, M., Kizil, U., Mirik, M., Smith, S. E., & Mendes, M. (2013). Determination of water stress with spectral reflectance on sweet corn (*Zea mays* L.) using classification tree (CT) analysis. *Zemdirbyste-Agriculture, 100*(1), 81–90.

Govender, M., Dye, P. J., Weiersbye, I. M., Witkowski, E. T. F., & Ahmed, F. (2009). Review of commonly used remote sensing and ground-based technologies to measure plant water stress. *African Journal, Water SA, 35*(5), 741–752.

Gröll, K., Graeff, S., & Claupein, W. (2007). Use of vegetation indices to detect plant diseases. In *Agrarinformatik im Spannungsfeld zwischen Regionalisierung und globalen Wertschöpfungsketten, Referate der 27. GIL Jahrestagung, 5.–7. März 2007, Stuttgart, Germany*.

Hoel, B. O., & Solhaug, K. A. (1998). Effect of irradiance on chlorophyll estimation with the Minolta SPAD-502 leaf chlorophyll meter. *Annals of Botany, 82*, 389–392.

IBM SPSS. (2012). *Decision trees 21 guide*. Copyright IBM Corporation 1989.

Kacira, M., Sase, S., Okushima, L., & Ling, P. P. (2005). Plant response-based sensing for control strategies in sustainable greenhouse production. *Journal Agricultural Meteorology, 61*, 15–22.

Katsoulas, N., Elvanidi, A., Ferentinos, K. P., Bartzanas, T., & Kittas, C. (2014). Calibration methodology of a hyperspectral imaging system for greenhouse plant water stress estimation. *Acta Horticulturae, 1142*, 119–126.

Katsoulas, N., Elvanidi, A., Ferentinos, K. P., Kacira, M., Bartzanas, T., & Kittas, C. (2016). Crop reflectance monitoring

as a tool for water stress detection in greenhouses: A review. *Biosystems Engineering, 151*, 374–398.
Katsoulas, N., Savvas, D., Tsirogiannis, I., Merkouris, O., & Kittas, C. (2009). Response of an eggplant crop grown under Mediterranean summer conditions to greenhouse fog cooling. *Scientia Horticulturae, 123*, 90–98.
Kim, Y., Glenn, D. M., Park, J., Ngugi, H. K., & Lehman, B. L. (2010). Hyperspectral image analysis for plant stress detection. In *Annual International Meeting, Paper Number 1009114*.
Kittas, C., Bartzanas, T., & Jaffrin, A. (2003). Temperature gradients in a partially shaded large greenhouse equipped with evaporative cooling pads. *Biosystems Engineering, 85*, 87–94.
Köksal, E. S. (2011). Hyperspectral reflectance data processing through cluster and principal component analysis for estimating irrigation and yield related indicators. *Agricultural Water Management, 98*, 1317–1328.
Lan, Y., Zhang, H., Lacey, R., Hoffmann, W. C., & Wu, W. (2009). Development of an integrated sensor and instrumentation system for measuring crop conditions. *Agricultural Engineering International: the CIGR Ejournal*. Manuscript IT 08 1115. Vol. XI.
Liaghat, S., & Balasundram, S. K. (2010). A review: The role of remote sensing in precision agriculture. *American Journal of Agricultural and Biological Sciences, 5*(1), 50–55.
Lichtenthaler, H. K., & Babani, F. (2000). Detection of photosynthetic activity and water stress by imaging the red chlorophyll fluorescence. *Plant Physiology and Biochemistry, 38*, 889–895.
Lichtenthaler, H. K., & Wellburn, A. R. (1983). Determinations of total carotenoids and chlorophylls a and b of leaf extracts in different solvents. *Biochemical Society Transactions, 11*, 591–592.
Loh, W. Y. (2011). Classification and regression trees. *Wiley Interdisciplinary Reviews: Data Mining and Knowledge Discovery, 1*, 14–23.
Lu, S., Lu, L., Zhao, W., Liu, Y., Wang, Z., & Omasa, K. (2015). Comparing vegetation indices for remote chlorophyll measurement of white poplar and Chinese elm leaves with different adaxial and abaxial surfaces. *Journal of Experimental Botany, 66*, 5625–5637.
Max, J. F. J., & Schurr, U. (2012). Greenhouse cover technology. *Hortucultural Reviews, 40*, 259–395.
Peñuelas, J., Gamon, J. A., Fredeen, A. L., Merino, J., & Field, C. B. (1994). Reflectance indices associated with physiological changes in nitrogen and water limited sunflower leaves. *Remote Sensing of Environment, 48*, 135–146.
Polder, G., van der Heijden, G. W. A. M., Keizer, P. L. C., & Young, I. T. (2003). Calibration and characterization of imaging spectrographs. *Near Infrared Spectroscopy, 11*, 193–210.
Ray, S. S., Das, G., Singh, J. P., & Panigrahy, S. (2006). Evaluation of hyperspectral indices for LAI estimation and discrimination of potato crop under different irrigation treatments. *International Journal of Remote Sensing, 27*, 5373–5387.
Sarlikioti, V., Driever, S. M., & Marcellis, L. F. M. (2010). Photochemical reflectance index as a mean of monitoring early water Stress. *Annals of Applied Biology, 157*, 81–89.
Schlemmer, M. R., Francis, D. D., Shanahan, J. F., & Schepers, J. S. (2005). Remotely measuring chlorophyll content in corn leaves with differing nitrogen levels and relative water content. *Agronomy Journal, 97*, 106–112.
Story, D., & Kacira, M. (2015). Design and implementation of a computer vision-guided greenhouse crop diagnostics system. *Machine Vision and Applications, 26*, 495–506.
Suárez, L., Zarco-Tejada, P. J., Berni, A. J., González-Dugo, V., & Fereres, E. (2009). Modelling PRI for water stress detection using radiative transfer models. *Remote Sensing of Environment, 113*, 730–744.
Sun, P., Grignetti, A., Liu, S., Casacchia, R., Salvatori, R., Pietrini, F., et al. (2008). Associated changes in physiological parameters and spectral reflectance indices in olive (*Olea europaea* L.) leaves in response to different levels of water stress. *International Journal of Remote Sensing, 29*, 1725–1743.
Taiz, L., Zeiger, E., Møller, I. M., & Murphy, A. (2015). *Plant physiology and development* (Sixth Edition). Companion Website published by Sinauer Associates.
Tsirogiannis, I. L., Katsoulas, N., Savvas, D., Karras, G., & Kittas, C. (2013). Relationship between reflectance and water status in a greenhouse rocket (*Eruca sativa mill.*) cultivation. *European Journal of Horticultural Science, 78*, 275–282.
Vogelmann, J. E., Rock, B. N., & Moss, D. M. (1993). Red edge spectral measurements from sugar maple leaves. *International Journal of Remote Sensing, 14*, 1563–1575.
Zarco-Tejada, P. J., González-Dugo, V., Williams, L. E., Suárez, L., Berni, J. A. J., Goldhamer, D., et al. (2013). A PRI-based water stress index combining structural and chlorophyll effects: Assessment using diurnal narrow-band airborne imagery and the CWSI thermal index. *Remote Sensing of Environment, 138*, 38–50.